Wind tunnel test and numerical study of a multi-sided wind tower with horizontal heat pipes

Energy 260 (2022) 125118

Contents lists available at ScienceDirect

Energy

journal homepage: www.elsevier.com/locate/energy

Wind tunnel test and numerical study of a multi-sided wind tower with horizontal heat pipes

Harry Mahon [a,*], Daniel Friedrich [a], Ben Hughes [b]

[a] School of Engineering, University of Edinburgh, Edinburgh, EH9 3DW, United Kingdom
[b] Department of Engineering, University of Hull, Hull, HU6 7RX, Yorkshire, United Kingdom

ARTICLE INFO

Keywords:
Passive ventilation
Wind tower
Wind tunnel testing
Computational fluid dynamics
Heat recovery
Heat pipes

ABSTRACT

Passive ventilation such as wind towers can ventilate spaces by using regional pressure differences and the stack effect. Wind towers are often closed throughout the winter to prevent an increase in heating energy demand. Heat pipes can be installed to transfer heat from the outgoing to the incoming air, however the inclusion of heat recovery can incur a pressure drop that negatively impacts ventilation rates. Here it is shown that with an array of horizontally arranged heat pipes, ventilation rates of 0.1 m^3/s are maintained at a 1 m/s inlet velocity. The incoming air temperature was raised by up to 2.8 °C, thereby increasing the operational window of the passive ventilation system. By mounting the heat pipes horizontally through the wind tower, direct heat transfer is facilitated between the inlet and outlet. The results demonstrate how a passive ventilation and heat recovery system is likely to operate in the winter months of a cooler climate according to the wind speed and temperature difference between the fresh and exhaust air. It is intended that this system will be further developed to provide both heating and cooling in the winter and summer respectively by installing a seasonal thermal loop.

1. Introduction

Buildings account for up to up to 40% of total energy demand worldwide [1]. With heat generation dominated by fossil fuels and cooling demand tripling since 1990 [2], there is significant scope to reduce the energy demand of heating, cooling, and ventilation (HVAC) systems in efforts to limit the global impacts of climate change. Indoor spaces are ventilated to prevent the buildup of pollutants, however, can result in increased energy demand through the use of fans and air-conditioning systems in order to maintain thermal comfort [3].

Wind towers are a form of passive ventilation adapted from the traditional Baud-Geer designs used throughout the Middle East for centuries [4]. Passive ventilation systems provide ventilation without any energy requirements by harnessing areas of relative positive and negative pressure as well as the stack effect [5]. Areas of positive pressure are created on the windward face of the wind tower, creating an area of relative negative pressure on the leeward side. This creates a combined driving and suction force through the ventilation system, replacing stale with fresh air (Fig. 1). The stack effect is caused by temperature differences within the room creating a buoyancy driven flow. Warm air rises naturally, passing through the ventilation outlet allowing cool air to flow in to replace it.

Despite the benefits of wind towers, these systems are often closed throughout winter as the introduction of unconditioned fresh air into the indoor environment results in an increase in heating energy demand. Consequently, they have been adapted from the traditional Baud-Geer designs, increasing the number of sides and louvres, changing the envelope shape, and installing heat recovery technology to improve performance [4,6–8]. During the winter months heat recovery devices can be transfer heat from the warm air flowing through the ventilation outlet to the cool air entering through the inlet. This results in an increase in incoming air temperature, limiting the increase in heating energy demand and lengthening the valid operational window of the passive ventilation system. Several reviews have explored heat recovery technologies for inclusion within passive ventilation, focusing on heat transfer rates, ease of integration, and incurred pressure drop [9,10].

In this study, heat pipes are mounted horizontally through the lower section of a multi-sided wind tower with the aim of recovering heat from the exhaust to the inlet air. Fig. 2 indicates the intended operation of the system. Throughout the winter air within an occupied building is heated actively and passively. Through ventilation much of this heat is lost to the environment and so energy is required to raise the fresh air

* Corresponding author.
E-mail address: A.h.mahon@sms.ed.ac.uk (H. Mahon).

https://doi.org/10.1016/j.energy.2022.125118
Received 29 March 2022; Received in revised form 30 June 2022; Accepted 9 August 2022
Available online 14 August 2022

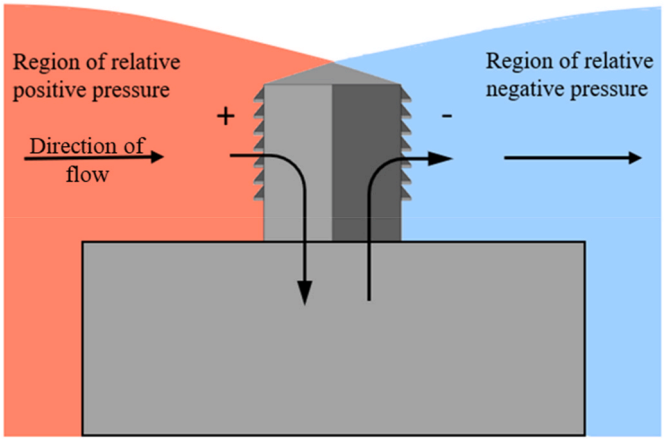

Fig. 1. Areas of relative positive and negative pressure created around a wind tower, a type of passive ventilation.

temperature to the comfort level of the building. Employing a wind tower and heat recovery system, cold air enters the wind tower guided by the external louvres with warm air simultaneously passing through the exhaust channels. As the exhaust air passes over the heat pipes through the outlet, the internal fluid evaporates. The vapour travels along the length of the pipe to the inlet where the passage of the cooler air causes it to condense, transferring the absorbed heat to the fresh air. It should be noted that 'cold' can also be effectively recovered between air streams in the summer via the reverse process, using internally cooled exhaust air as a heat sink for heat removed from the warm air flowing through the inlet, however for the purpose of this study the focus will remain on operation during the winter months.

The wind tower used is a commercially available design developed through several studies [11,12]. This system looks to iterate upon previous designs by reducing the overall number of heat pipes within the wind tower whilst maximizing direct heat transfer between air streams, crucially maintaining a minimum inlet flow rate of 10 L/s per occupant [3]. By orientating the heat pipes horizontally, it is intended that future design iterations will be better able to remove and deliver heat to and from the heat pipes through a seasonal heat transfer loop [13].

To evaluate the performance of the wind tower and heat recovery system, a full-scale wind tunnel test was conducted at the Building Research Establishment (BRE), UK, with the results used to validate a numerical model. The numerical model was developed using the commercial code ANSYS Fluent, first creating a 3D CAD model of the experimental geometry and then discretising it through a meshing process. After verifying the accuracy of the numerical model through a mesh independence study and validating the results against the experimental measurements, a range of boundary conditions were applied to the model to establish the potential for heat recovery to increase the incoming air temperature. Finally, an energy analysis is performed to estimate the energy saved due to heat recovery through the wind tower.

In contrast to previous works exploring the application of vertical heat pipes through a multi-sided wind tower [6], and horizontal heat pipes through a single sided wind tower [14], this paper seeks to determine the potential for thermosyphon heat pipes oriented horizontally through the base of a multi-sided wind tower. The performance of the heat pipes is evaluated at temperatures chosen to represent a mild-cold climate whereas often much larger temperature differences are explored.

This study further builds upon previous scale model experiments by conducting a full-scale wind tunnel test of a multi-sided wind tower. By conducting the test at full-scale, the performance of the thermosyphon heat pipes is directly evaluated. This also allows the experimental temperature readings to be used to validate the heat pipe modelling approach in addition to velocity measurements, where typically only velocity is used. Through this the aim is limit the total number of heat pipes within the wind tower, decreasing the overall weight and cost of the system whilst maintaining ventilation and heat recovery rates.

2. Previous related work

2.1. Passive ventilation and CFD studies

Passive ventilation can lead to indoor heat loss [15]. In response, various heat recovery technologies have been explored for use within ventilation to recover waste heat [6,16–19]. Within passive ventilation systems driving pressures can be very low and so overly obstructing the air flow can impinge on ventilation rates. Therefore, wind tunnel testing is often employed alongside Computational Fluid Dynamics (CFD) modelling to evaluate the impact of installed heat recovery devices prior to commercial application.

While early work using traditional Baud-Geer wind tower designs focused on the use of evaporative cooling [20], a study comparing evaporative cooling with heat pipes determined that while both methods could reduce incoming air temperature by up to 15 °C in hot climates, the lower water requirements for the closed heat pipe system made them more favorable [21]. Further research compared the use of heat recovery technologies such as heat pipes, rotary thermal wheels, plate heat exchangers, and run arounds within passive ventilation systems. Heat pipes and rotary wheels were found to be desirable due to their high rates of heat transfer and low incurred pressure drops [10].

Shao and Riffat [22] investigated the flow loss caused by heat pipes within stack flow. The results showed that for a heat recovery efficiency

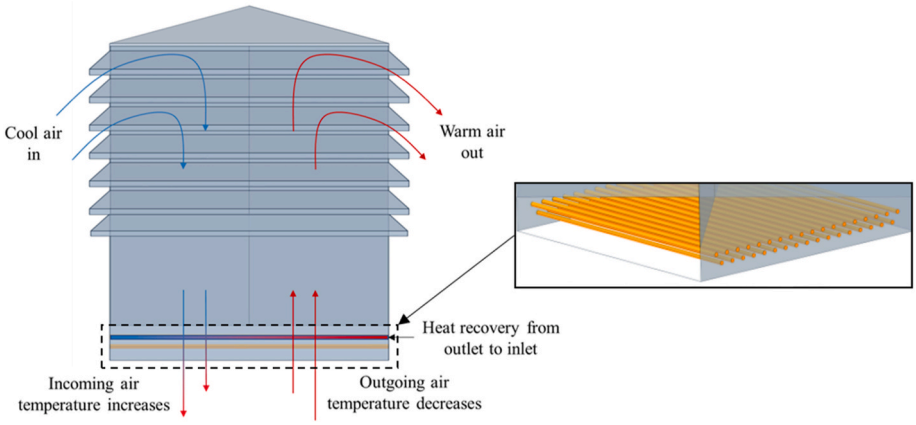

Fig. 2. Heat recovery between the inlet and outlets of a multi-sided wind tower.

of 50% and a flow speed of 0.5 m/s, the pressure loss over the heat pipe array was around 1 Pa, indicating little effect on the performance of temperature driven flow. Riffat and Gan [23] then built an array of heat pipes within a chimney stack to determine the heat recovery effectiveness. It was shown that with increasing air velocity the effectiveness of the heat pipe decreases, with an increase in the number of banks of heat pipes simultaneously increasing effectiveness and the pressure drop.

Hughes et al. [24] later used CFD modelling to evaluate how the distance between the pipes in an array affects heat transfer and low rates. Using a horizontal distance of 0.05 m between heat pipes in a row and a pitch of 0.035 m was found to be optimum, establishing a 15.6 °C temperature reduction for the incoming air in a hot, dry climate, and 3.3 °C of pre-heating for cool incoming air in a mild climate.

Calautit et al. [14] explored the use of heat pipes within a single sided wind tower featuring a cool sink. Compared against a benchmark model without heat pipes, the average internal airspeed of 0.49 m/s was reduced by 40.8% once they were introduced. The cooling effectiveness was found to decrease with increasing wind speed, with only 6 °C of cooling achieved at 5 m/s inlet speed compared with 9.5–12 °C at between 1 and 2 m/s inlet speed respectively.

A further study explored the use of vertically arranged heat pipes within a multisided wind tower [6]. The wind tower was capable of supplying air to the room at over 10 L/s per person for external wind speeds greater than 1 m/s, with the heat pipes raising the incoming air temperature by 4.5 K when the surface of the heat pipe was set at 293 K. Although increasing the number of rows of heat pipes from 1 to 3 improves thermal performance, inlet and outlet velocities were reduced.

2.2. Heat pipe modelling approach

Due to the phase change cycle within heat pipes, modelling them accurately using CFD can be challenging and as a result several differing approaches have been developed.

Alizadehdakhel et al. [25] used a volume of fluids method to model a single thermosyphon heat pipe in a 2D computational domain. Although this method is perhaps the most accurate at modelling the phase change cycle within the heat pipe, the simulation is conducted at extremely small time-steps ($<10^{-3}$ s) in only 2 dimensions and therefore is not considered suitable for this case.

Calautit et al. [15] applied a constant surface temperature to an array of vertically arranged heat pipes within a three-dimensional numerical model to predict the increase in incoming air temperature achievable when using a heat pipe and heat source system. When the temperature of the heat pipes was 20 °C, the fresh air temperature was raised by 4.5 °C.

Hughes et al. [26] explored a multi-phase flow with coupled heat and mass transfer in horizontally arranged heat pipes. A three-dimensional model was used to predict the effectiveness of the heat pipes, validating the model against an earlier experimental study. Achieving 15.6 °C of pre-cooling and 3.3 °C of pre-heating, the ability for thermosyphon heat pipes to operate horizontally is highlighted.

Mroue et al. [27] and Ramos et al. [28] approximated the heat pipe as a solid conducting body by deriving the total thermal resistance of a heat pipe during heat transfer. The total thermal resistance is the sum of the resistances from conduction and convection at the evaporator and condenser, as well as the resistances from the boiling, pressure change, and condensation of the heat transfer fluid.

2.3. Wind tunnel test geometry

A full-scale wind tower test was conducted using an environmental chamber at the BRE, UK. A test room (3.5 × 2.3 × 2.2 m) was built centrally within an environmental chamber (11.0 × 6.6 × 3.68 m), with a hole cut through the centre of the roof and the wind tower aligned over it (Fig. 3). Four fans with a frontal area of 4 × 1.4 m were installed to convert the upper section of the environmental chamber into a wind tunnel test section. Walls were erected either side of the test room in line

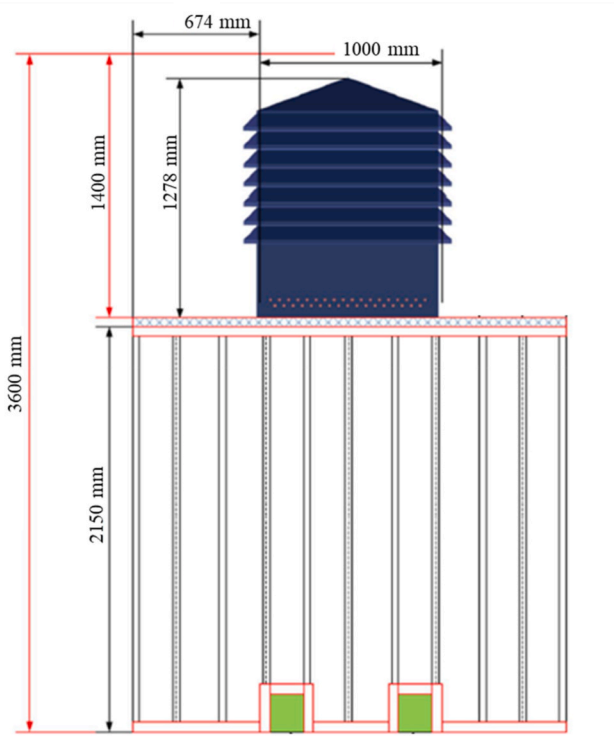

Fig. 3. Test room and wind tower dimensions within the larger environmental chamber.

with the outer edges of the fan array to constrain the flow of air around the wind tower. Given the scale of the system, the fans were only large enough to draw air over the wind tower rather than the entire test room (Fig. 4). Inside the test room a 12 kW gas boiler feeding a heated coil was deployed to provide heating. Air was drawn across the heated coils by two inline fans and discharged into the room via semi-rigid ducts and supply plenums.

The commercial wind tower design measures 1 × 1 × 1.28 m, featuring seven external louvres on each side and an internal cross-frame dividing the structure into four equal quadrants. Each quadrant can perform as an inlet or an outlet depending upon the incident wind direction. For this experiment the wind tower was orientated with one quadrant facing windward to act as the inlet, with the remaining three as outlets. A total of 35 water-filled thermosyphon heat pipes were installed in 2 rows across the base of the wind tower perpendicular to the direction of flow. Fig. 5 indicates the horizontal and vertical rake between heat pipes alongside the base dimensions of the wind tower, where D, S_t, and S_L equal 16, 35, and 50 mm respectively.

2.4. Measurement techniques

Initial inlet velocities between 1 and 6 m/s were applied to establish the impact of heat pipes on the inlet mass flow without considering the temperature of the flow. Subsequently inlet velocities of 2 and 4 m/s, inlet temperatures of 5 and 10 °C, and outlet temperatures of 24, 27, and 30 °C were used to study the potential pre-heating of incoming air through heat recovered from the outgoing air. A TSI 8475 omnidirectional spherical hot bead anemometer was used to take velocity measurements, with an uncertainty of ±3% of the reading. Temperatures were recorded using thermocouples with an uncertainty of ±1% at 25 °C. Velocity readings were taken over 2 min periods and averaged at each point. Temperature readings are given as the average reading over an hour under steady state conditions.

When performing wind tunnel testing, the placement of a bluff body in the flow can result in increased wind speeds in areas where the flow is

Fig. 4. Wind tunnel experimental set up.

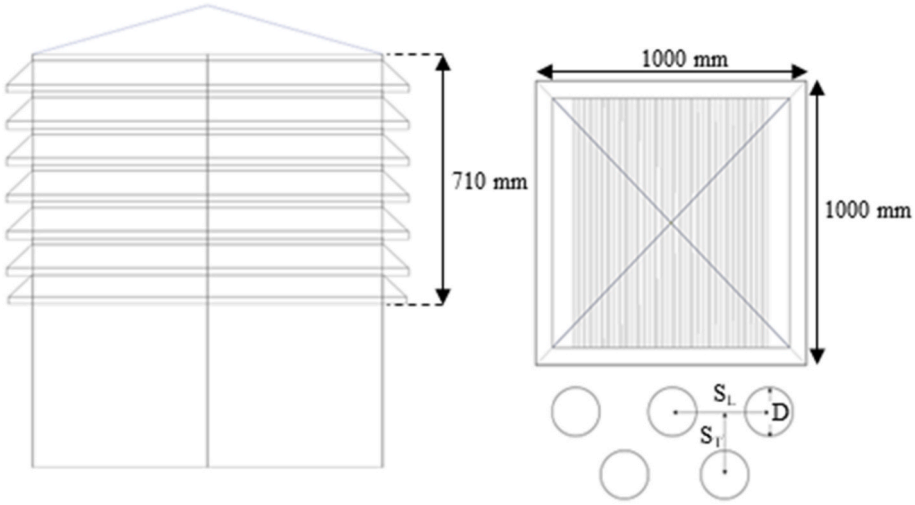

Fig. 5. Heat pipe spacing and wind tower dimensions.

constricted due to the walls of the wind tunnel test section. The degree to which the results are affected is defined by the blockage ratio, found by dividing the frontal area of the test object by the cross-sectional area of the wind tunnel. Using the ratio of the frontal area of the wind tower to that of the fans, the blockage ratio is calculated to be 23.3%. Although this is above the 10% recommended [29], given the scale of the wind tower, increasing the size of the fans to reduce the blockage ratio below 10% was not practical. The inlet velocity through the wind tower was measured 0.8 m upwind of the inlet quadrant and this is the speed reported, approximating free wind speed, and therefore no corrections were made.

2.4.1. Volumetric flow rate

The inlet quadrant of the wind tower is divided into six approximately equal areas and the wind speed measured at the centre of each. The total volumetric flow rate through the inlet was then calculated according to the equation:

$$Q_v = \sum_{i=1}^{n} A_i \times U_i \quad (1)$$

where Q is the flow rate through the entire quadrant, A_i is the area of point i, and U_i is the velocity measured at the centre of point i. Fig. 6 shows the position of points A – F with measurements taken over 2 min and averaged.

2.4.2. Temperature data

To evaluate the performance of the heat pipes, temperature measurements were taken at points above and below the heat pipes through the inlet. Due to significant variations in air velocity across the inlet, temperature measurements were taken in two lateral regions of the upwind quadrant (Fig. 7). The average of points 1 and 2 was then averaged against the value at point 3 to find the overall average temperature increase.

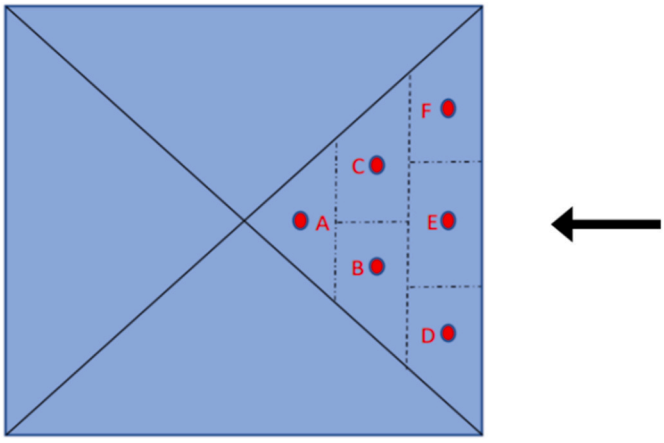

Fig. 6. Inlet quadrant area divisions and measurement points.

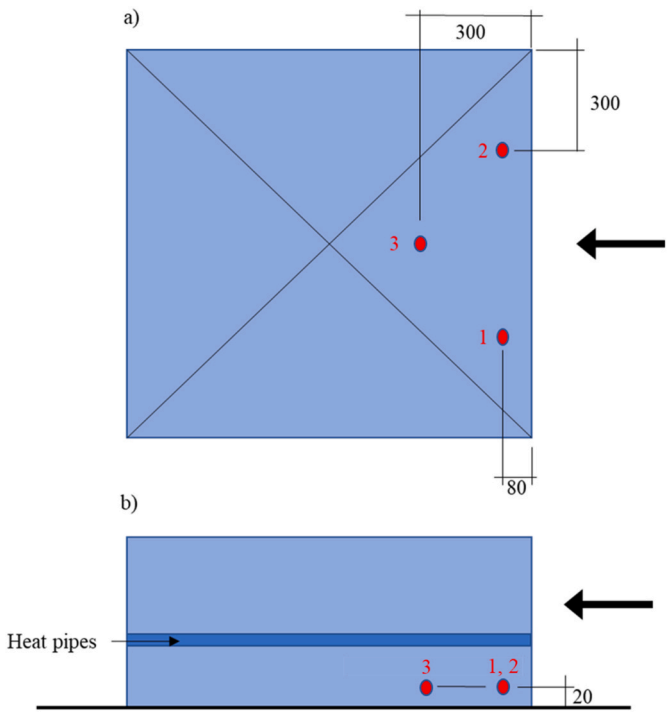

Fig. 7. - a) top-down view of temperature sensor locations b) side view of temperature sensor locations. Arrow indicates direction of flow.

2.5. Numerical methodology

The commercial CFD software ANSYS Fluent 20 was used to simulate the air flow through the wind tower model. The simulation was a full-scale, three-dimensional replica of the experimental set up described in Section 3.0. Fluent uses the Finite Volume Method (FVM) with a Semi Implicit Method for Pressure Linked Equations (SIMPLE), velocity-pressure coupled solver. For the FVM the computational domain must first be split into many smaller elements that constitute the mesh, with the values of each variable calculated at the centre of the element. The k-ε turbulence model with standard wall functions is applied to resolve the turbulent elements of the air flow as is common in passive ventilation applications [6,30,31]. The governing equations used to determine the values throughout the computational domain including the conservation of mass, energy, and momentum, as well as turbulent kinetic energy and energy dissipation rate can be found in the ANSYS Fluent Theory Guide [32], and are summarized in Ref. [33]. All simulations were performed under steady state conditions.

2.6. Geometry

The wind tower and heat pipes were modeled using Autodesk Inventor before being imported into the ANSYS workbench. Here the fluid volumes within the boundaries of the test room and wind tunnel test section were extracted to create two separate fluid regions coupled via a boundary through the base of the wind tower. Fig. 8 shows the final geometry of the wind tower, heat pipes, test room, and wind tunnel test section. The fluid representing the wind tunnel test section measures $10.5 \times 4 \times 1.4$ m while the fluid volume extracted from the test room measures $3.5 \times 2.3 \times 2.1$ m. As the computational model is at a 1:1 scale with the wind tunnel test, geometric and dynamic similarity is achieved and therefore no scaling of inlet velocity or temperature is necessary.

2.7. Mesh design

When discretising the model geometry to create the mesh, a larger number of mesh elements will generate more accurate results but will also take longer to compute. Both the wind tunnel test section and test room fluids were divided into smaller volumes. In doing so, the number of divisions along each edge can be controlled, enabling better connections between volumes with differing element types (Fig. 9). Given that the wind tower is a relatively complex geometry, an unstructured mesh was used with size functions applied throughout to control the size of the mesh elements in regions such as the louvres and heat pipes [15]. Away from the wind tower, a structured mesh was used, reducing the total number of mesh elements whilst allowing a comparatively finer mesh than if tetrahedral elements had been applied in the same areas.

Wall functions are used within ANSYS to model the laminar sublayer of the flow in the near wall region. The y^+ value can be used to find the appropriate thickness of near wall elements to accurately capture the flow properties through the wall functions. Inflation layers were used on the surface of the heat pipes and wind tower to control the thickness of the cells adjacent to the walls, with the y^+ value ideally falling between 30 and 300 when using standard wall functions [34].

2.7.1. Heat pipe modelling approach

Using flow properties derived from the experimental velocity and temperature data, the overall heat transfer coefficient of the heat pipe was calculated according to the process laid out in Refs. [27,28], modelling each heat pipe as a solid conducting body. In early simulations the pre-heating of the incoming air achieved through this method

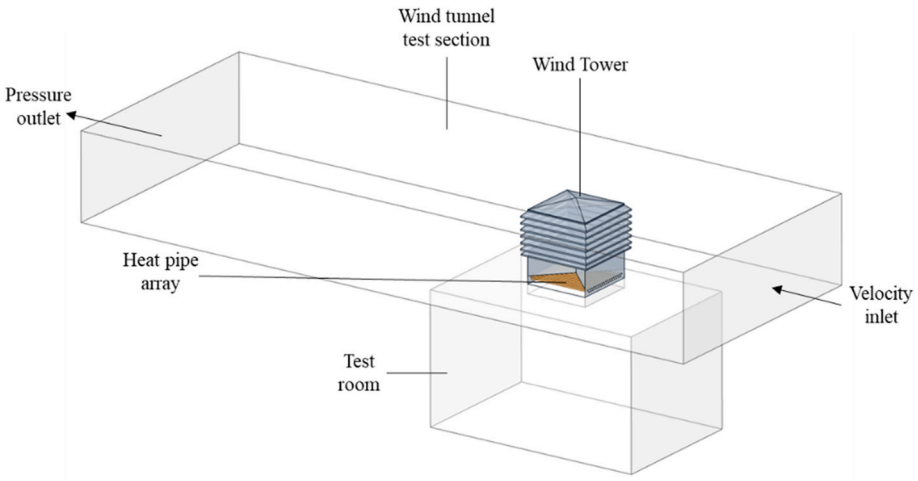

Fig. 8. Geometry used within ANSYS Fluent.

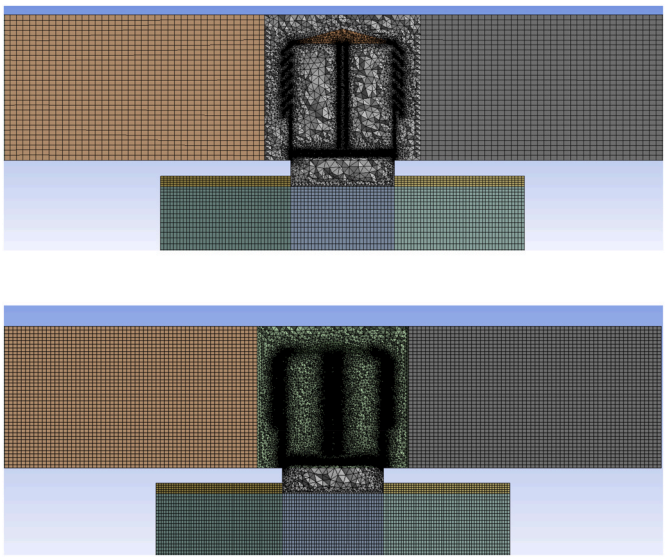

Fig. 9. Cross section of increasing mesh cell density from medium (Top) to fine (Bottom) grid resolution.

was however drastically lower than the results recorded during the wind tunnel test. This is potentially due to the relatively low temperature difference between the evaporator and condenser sections of the wind tower when compared with other papers that have employed this method.

As a result, the method as described by Calautit et al. [15] was employed, assuming a constant surface temperature along the length of the heat pipe and applying this as a boundary condition within the simulation to the heat pipe geometry. The average surface temperature of the heat pipe is assumed to be equal to the average temperature of the heat source, which in this case is the warm outgoing air passing through the outlets of the wind tower. Although applying surface temperature as a boundary condition is an oversimplification of the heat transfer process along the length of the heat pipes, as is shown in Section 5.0, the difference between the CFD and experimental results indicate that this method can provide a reasonable estimation of the pre-heating of the inlet air achieved through heat recovery.

2.7.2. Mesh independence study

To verify the results of the generated mesh, a mesh independence study was undertaken to assess the numerical error and uncertainty of the calculations. Sofotasiou [35] laid out one method to determine the accuracy of the results using a minimum of three mesh sizes which is repeated below.

The Grid Convergence Index (GCI) was developed by Roache [36], using Richardson Extrapolation to find the discretisation error based upon a series of meshes increasing in size with a constant grid refinement ratio and uniform order of accuracy in space and time [35]. Equations (2) and (3) can be used to determine the discretisation error in coarse and fine grids respectively:

$$E_2[coarse\ grid] = r^{p} * \varepsilon_{32} / (r^{p} - 1) \tag{2}$$

$$E_1[fine\ grid] = \varepsilon_{21} / (r^{p} - 1) \tag{3}$$

where $E_{1,2}$ are the coarse (E_2) and fine (E_1) grid Richardson error estimators, r is the grid refinement ratio, p is the order of accuracy equal to the order of the discretisation scheme, and ε indicates the difference in numerical solution in progressively finer grids:

$$\varepsilon_{32} = (\varphi_3 - \varphi_2)/\varphi_2 \tag{4}$$

$$\varepsilon_{21} = (\varphi_2 - \varphi_1)/\varphi_1 \tag{5}$$

where $\varphi_{3,2,1}$ are numerical solutions generated at the same point in coarse, medium, and fine grids, respectively. While the grid refinement ratio is ideally equal to 2 applied consistently over the entire mesh this is not always practical. For scenarios where r and p are not equal to 2, Roache [37] later introduced a safety factor, using equations (5) and (6) to calculate the GCI index for coarse and fine grids:

$$GCI_{21}^{fine} = F_s\,|E_1| \tag{6}$$

$$GCI_{32}^{coarse} = F_s\,|E_2| \tag{7}$$

where $F_s = 1.25$ is commonly applied [38]. In the case that the refinement ratio between the coarse - medium and medium - fine grids is equal, the value of r is calculated according to equations (8) and (9):

$$r_{21} = (N_1/N_2)^{1/D} \tag{8}$$

$$r_{32} = (N_2/N_3)^{1/D} \tag{9}$$

where N_3, N_2, and N_1 are the number of cells in the coarse, medium, and fine grids respectively, and D is the dimensionality of the model (D = 3 for a 3D model). The order of the solution can be calculated according to equation (10) when r is constant or equation (11) when not [35,39]:

$$p = \frac{ln\,(\varepsilon_{32}/\varepsilon_{21})}{\ln(r)} \tag{10}$$

$$p_k = \frac{ln\,(\varepsilon_{32}/\varepsilon_{21})}{\ln(r_{21})} + \frac{1}{\ln(r_{21})}\,[\,ln(r_{32}^{p_k} - 1) - ln(r_{21}^{p_k} - 1)] \tag{11}$$

where p_k is calculated iteratively, with the first value equal to the best guess. The extrapolated values and resulting extrapolative error can then be found using the following equation:

$$\varphi_{21,ext} = (r_{21}^{p}\varphi_1 - \varphi_2)/(r_{21}^{p} - 1) \tag{12}$$

In the present case, three grids of 39, 029, 483, 22, 487, 165, and 12, 513, 490 were used to calculate the GCI index and resulting discretisation errors. Velocities were measured in each grid at three points 0.15, 1.05, and 1.95 m below the centre of the wind tower inlet. Table 1 illustrates the results of the mesh independence study. Using the calculated GCI_{fine}, the numerical uncertainty ranged between 3.70% and 6.88%, corresponding to a maximum of ±0.018 m/s at the point 1.95 m below the wind tower inlet.

2.8. Cell zone and boundary conditions

Initial boundary conditions equivalent to those of the wind tunnel test were used to verify the accuracy of the numerical model in predicting velocity and temperature changes through the wind tower. Inlet

Table 1
Calculations used to find discretisation error between the coarse, medium, and fine mesh.

Height	0.15 m below inlet	1.05 m below inlet	1.95 m below inlet
N1, N2, N3	39,029,483, 22,487,165, 12,513,490	39,029,483, 22,487,165, 12,513,491	39,029,483, 22,487,165, 12,513,492
r_{21}	1.22	1.22	1.22
r_{32}	1.20	1.20	1.20
φ_3	1.38	1.12	0.34
φ_2	1.31	1.02	0.27
φ_1	1.27	0.97	0.26
Pk	3.88	3.88	3.88
$\varphi_{21,ext}$	1.23	0.93	0.25
$\varphi_{21,ext}$ error	2.96%	4.21%	2.37%
e_{21}	2.98%	4.19%	2.41%
GCI_{fine}	3.60%	5.26%	6.88%

velocities of 1.33, 2.02, 4.17, and 5.96 m/s were simulated using a uniform velocity profile. Enabling the energy equation, inlet conditions of 2 m/s and temperatures of 5 and 10 °C were then applied with heat pipe surface temperatures of 24, 27, and 30 °C.

Following the validation, the inlet velocity was varied between 1 and 5 m/s for wind tower models featuring 1–3 rows of heat pipes, investigating the impact of an increasing number of heat pipes on inlet mass flow rate. To evaluate the potential for pre-heating of the incoming air, constant surface temperatures of 24, 27, and 30 °C were applied to the walls of the heat pipes, equal to the outlet air temperatures reached during the wind tunnel test [6,15,21,24]. Inlet temperatures of 5 and 10 °C were applied.

2.9. Criteria for solution convergence

ANSYS Fluent uses the finite element method to iteratively solve partial differential equations throughout the discretised domain. Residuals are used to indicate the error throughout the model, where a higher residual indicates a worse solution. The default convergence criteria deem the solution to have converged when the monitor for each residual falls below 10^{-6} for the energy equation and 10^{-3} for all other equations [32]. This however does not occur in all cases and convergence can be judged by the individual by monitoring the residuals to evaluate if the values throughout the model are still changing with each iteration of the simulation. After early simulations found that convergence was not occurring according to the pre-determined parameters of the program, monitor points were placed at areas of interest within the computational domain. These monitors measured the incoming and outgoing velocity and temperature through the wind tower, with convergence deemed to have been achieved once the value at each point remained unchanged for at least 500 iterations [5].

3. Validation

Comparisons between the recorded values from the wind tunnel test and CFD simulations are used to validate the computational model. To deem the model validated, the percentage error between the two datasets must fall into an acceptable range.

3.1. Velocity

Once the simulation has converged the velocity is measured at 6 points below the heat pipes and the values recorded compared with those taken during the wind tunnel test. Table 2 compares the results from the experiment and CFD model in the inlet quadrant of the wind tower for four inlet velocities. The largest velocity is seen at point A and the lowest at points D and F consistently across both the experimental and numerical results. The lower velocities at points D and F result from areas of recirculation above the heat pipes. These are created as the air flows over the louvres into the inlet quadrant and makes contact with the x-frame towards the corners of the wind tower. The fast-moving air is naturally guided towards the centre of the wind tower by the angle of the x-frame, leaving pockets of slow-moving air in which recirculation occurs. This results in a slower velocity over the heat pipes in these regions, increasing short circuiting and lowering the recorded velocities at points D and F (Fig. 10). Conversely, through the centre of the inlet inline with points A and F there are little disruptions to the flow and therefore the velocity before and after the heat pipes is much higher. The average error across the measurement points for each inlet velocity varies from 11.0 to 37.9%, however as both sets of results follow the same general trend the accuracy is considered sufficient to validate the CFD model as has been established in past works covering wind tunnel testing of passive ventilation [11,40,41].

Comparing the mass flow rate through the wind tower inlet (Table 3), there is a consistent over-estimation. Overestimating the inlet mass flow rate through the inlet is likely to lead to an underestimation of heat transfer to the fresh air, although as the velocities are low this will not be significant.

By dividing the measured velocity at each point by the inlet velocity (U_{ref}), the dimensionless velocity can be calculated. When comparing the dimensionless velocities at each point in relation to the inlet velocity, the behaviour of the CFD results is very predictable in comparison to the experimental results (Fig. 11). Observing where the largest differences are seen in the results at points D and F, these points are likely to be in the vicinity of areas recirculation for which the limitations of the k-ε wall function equation in modelling have been acknowledged [42,43]. Looking at the measured experimental velocity at point E with an inlet velocity of 5.96 m/s, the value recorded is far below the expected value provided it was consistent with the other inlet velocities, and therefore the error is much higher. Considering the measured velocities at each of the other points are consistent with previous trends, it is deemed that this likely resulted from errors made during the measuring process. The U/U_{ref} value at each point remains stable as the inlet velocity increases for the CFD results, whilst the variation in the experimental results is much greater. This highlights the predictable nature of the flow through the CFD model, whereas the wind tunnel flow is much more variable resulting in differences in the recorded values.

Table 2
Experimental vs CFD results used to validate the computational model.

Inlet Velocity	1.33 m/s			2.02 m/s		
Point	Experimental (m/s)	CFD (m/s)	% Error	Experimental (m/s)	CFD (m/s)	% Error
A	0.90	0.94	4.76	1.20	1.50	25.36
B	0.80	0.88	10.31	1.00	1.32	32.36
C	0.70	0.77	10.56	1.20	1.20	0.02
D	0.50	0.43	13.82	0.70	0.65	7.29
E	0.80	0.72	9.48	1.10	1.12	1.75
F	0.50	0.41	17.06	0.60	0.63	5.76
Average error			11.00			12.09
Inlet Velocity		4.17 m/s			5.96 m/s	
Point	Experimental (m/s)	CFD (m/s)	% Error	Experimental (m/s)	CFD (m/s)	% Error
A	2.60	3.19	22.84	3.90	4.59	17.70
B	1.80	2.79	55.21	3.00	4.02	33.88
C	2.20	2.55	15.99	3.40	3.64	7.15
D	0.90	1.35	49.50	1.40	1.95	39.26
E	2.00	2.36	18.17	1.70	3.40	100.04
F	0.80	1.32	65.37	1.60	1.90	18.77
Average error			37.85			36.13

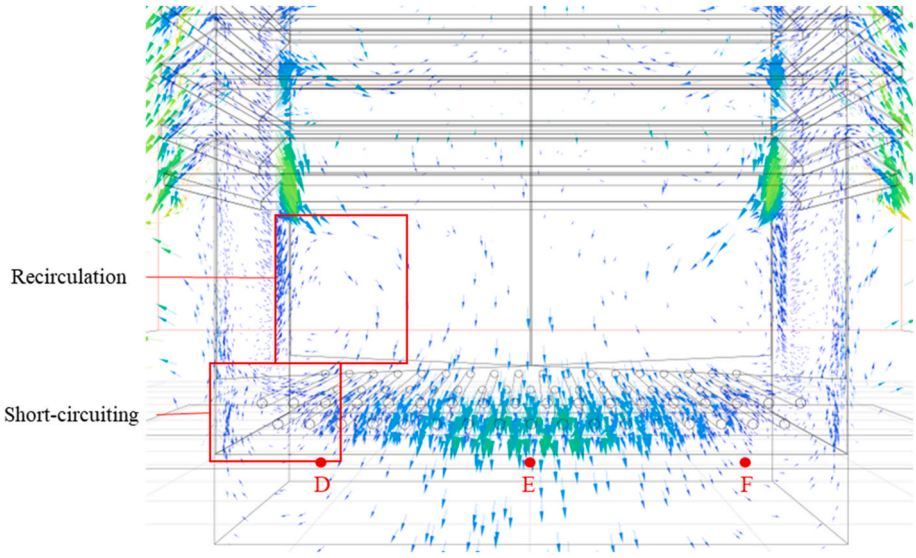

Fig. 10. Vectors of velocity through the wind tower. Plane intersects points D, E, and F showing areas of recirculation and short-circuiting.

Table 3
Comparison of mass flow rate through wind tower inlet.

Inlet Velocity (m/s)	Inlet mass flow rate (m^3/s)		
	Experimental	CFD	% Error
1.33	0.17	0.17	2.13
2.02	0.21	0.27	21.62
4.17	0.41	0.57	27.49
5.96	0.6	0.81	26.15

3.2. Temperature

Fig. 12 compares the pre-heating of the fresh air during the wind tunnel test and CFD simulation against the difference in temperature between the fresh air and heat pipes. The average error between the datasets is 6%, with a maximum difference of 12.77% or 0.21 °C when using a heat pipe temperature of 27 °C and inlet conditions of 5 °C and 2 m/s. When plotting a line of best fit for the experimental results it is seen that the CFD results match up almost exactly along this trend.

4. Results and discussion

Following the validation of the computational model, simulations using the boundary conditions described in section 4.3 were undertaken.

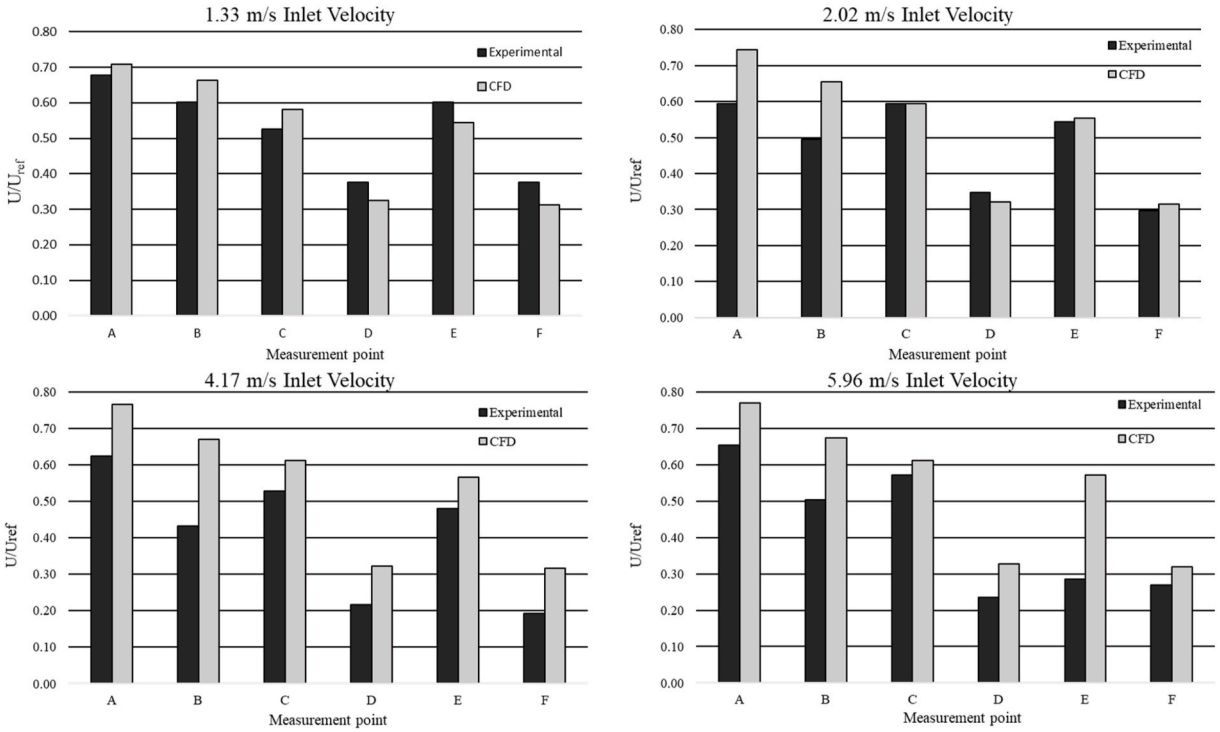

Fig. 11. U/U_{ref} at velocity measurement points below heat pipes for experimental and CFD results.

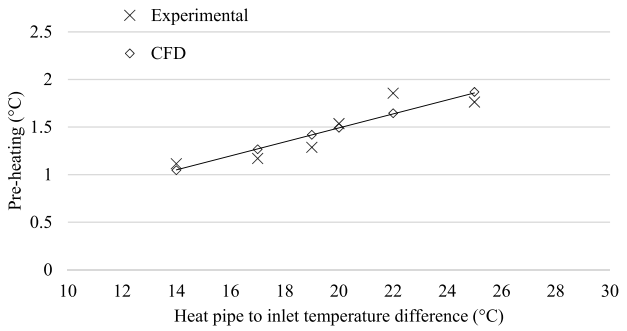

Fig. 12. Experimental vs CFD results for pre-heating of incoming air with inlet temperatures of 5 °C.

The effect of inlet velocity, heat pipe temperature, and the number of heat pipes on ventilation rates and pre-heating of fresh air were explored.

4.1. Ventilation rates

Fig. 13 shows the effect of increasing the number of rows of heat pipes on the inlet mass flow rate of the wind tower. An increasing number of heat pipes through the wind tower is found to be indirectly proportional to the inlet mass flow rate, with an average decrease of 18.6% from 1 to 2 rows and 9.4% from 2 to 3. The reduced impact of an additional row of heat pipes between 2 and 3 rows is thought to be due to the staggered arrangement. When increasing the number of rows from 1 to 2, the blockage of the inlet channel increases proportionally by a much greater amount than from 2 to 3, considering that rows 1 and 3 are in line with one another. This insinuates that additional rows of heat pipes could be installed without a significant detrimental effect to the inlet mass flow rate. Slower velocities over the heat pipes also allow more time for heat transfer to take place from the surface of the heat pipe to the incoming air. A single wind tower with 3 rows of heat pipes at an average inlet velocity of 4 m/s provides sufficient ventilation to achieve 6 ACH in a space with an approximate volume of 290 m^3.

Fig. 14 shows the contours of velocity through the wind tower model. Here the increase in air speed due to the narrowing of the channel over the roof of the wind tower is apparent. The air moving in through the inlet flows into the room below, hitting the floor and then distributing throughout the room. The use of a diffuser would further increase the distribution of fresh air and prevent a draught directly below the inlet of the wind tower. A small amount of short circuiting is observed between the inlet and the outlets. The use of automated dampers would allow the flow of air to be cut off in the case that wind speeds or temperatures were outside of a pre-determined acceptable range.

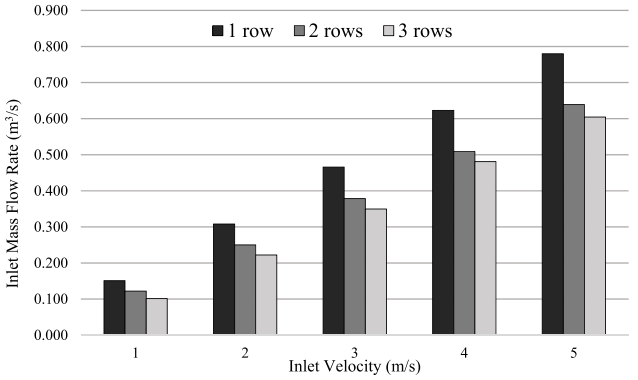

Fig. 13. Change in inlet mass flow rate with increasing inlet velocity and number of heat pipes.

4.2. Thermal performance

Fig. 15 indicates the average fresh air temperature increase for wind towers with 1–3 rows of heat pipes at inlet velocities of 2 and 4 m/s. Again, heat pipe temperatures of 24, 27, and 30 °C and inlet temperatures of 5 and 10 °C were applied, presented as the temperature difference between the two. Pre-heating is found to be indirectly proportional to the number of heat pipes and directly proportional to the difference in temperature between the inlet and heat pipe surface. Increasing inlet velocity also serves to reduce the amount of pre-heating as would be expected.

Using three rows of heat pipes with a temperature difference of 25 °C between the fresh air and the heat pipes the incoming air temperature was raised by 2.80 °C and 1.75 °C for inlet velocities of 2 and 4 m/s respectively. Both inlet velocity and the number of heat pipes have a significant impact on the level of pre-heating. Although increasing the number of heat pipes reduces the inlet mass flow rate, as the velocity through the inlet is reduced the contact time between the fresh air and the heat pipes is increased, therefore increasing total heat transfer.

A temperature contour of the flow through the wind tower inlet is shown in Fig. 16 featuring two rows of heat pipes with inlet conditions of 5 °C and 2 m/s. Pre-heating of the fresh air increases towards the outer edges of the heat pipe array where the velocity is lower, however the flow is subject to some short-circuiting between the inlet and outlets due to their proximity at these points. A slight increase in the air temperature above the heat pipes can be observed due to an area of recirculation close to the wind tower wall where the plane was situated. The temperature of the air through the outlets would be expected to decrease as heat is transferred from the air to the heat pipe, causing the heat pipe internal fluid to evaporate.

When comparing the performance of the heat recovery system against that of similar studies, it is found to be similar to that of a rotary thermal wheel when operating at a similar temperature difference between the inlet and outlet [7], and marginally below that of a wind tower with vertically arranged heat pipes [15]. By orienting the heat pipes vertically there is a larger surface area available for heat transfer, however this design requires an intermediary system linking the heat pipes through the inlet and the outlets. In the current case, the addition of fins could be used to increase the available surface area for heat transfer, however, will further limit the flow of air through the wind tower.

In cases such as this where the wind direction results in a single inlet and three outlet quadrants, straight heat pipes are sufficient to transfer heat from the outlet to the inlets. However, under atmospheric boundary conditions where the wind direction is constantly changing a combination of curved and straight pipes might be more practical to ensure that heat is effectively transferred from the outlets to the inlets regardless of wind direction. Although the current study did not evaluate the effects of an atmospheric boundary layer inlet condition onto the wind tower, previous investigations featuring similar wind tower designs have found that ventilation performance decreases, largely due to flow separation at the leading edge of the building.

4.2.1. Heating demand

The heating energy reduction associated with the pre-heating of fresh air can be estimated by finding the energy required to raise the temperature of the fresh air to that of the internal air temperature and comparing it against the baseline case with no pre-heating:

$$Q_H = Q_v \, \rho \, C_p \, \Delta T \tag{13}$$

where Q_H is the energy required in watts, Q_v is the volumetric flow rate of the air through the inlet of the wind tower, ρ is the density, C_p is the specific heat capacity, and ΔT is the temperature difference between the air and the proposed internal air temperature post heat pipes.

Fig. 17 below shows the expected reduction in energy demand in

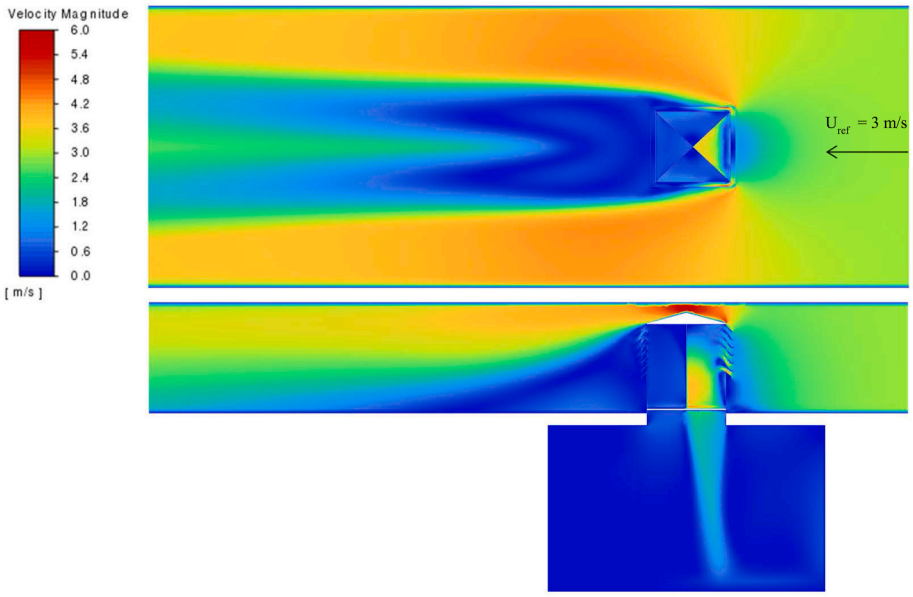

Fig. 14. Contours of velocity through the midplane of the wind tunnel test section and test room with 2 rows of heat pipes.

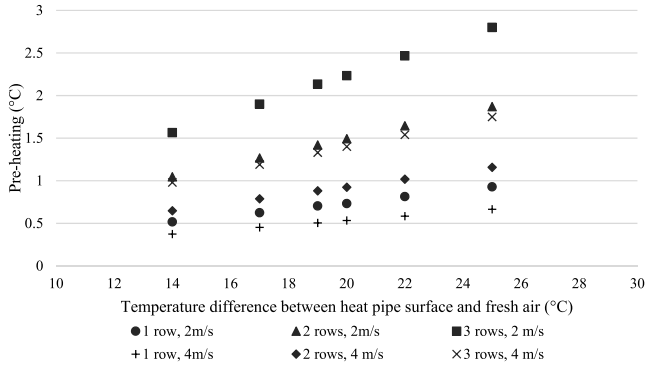

Fig. 15. Fresh air temperature increase compared to temperature difference between the fresh air and heat pipes.

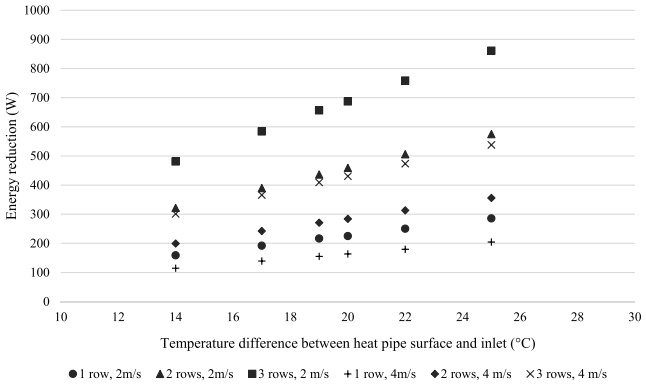

Fig. 17. Energy saving in watts due to pre-heating of incoming air.

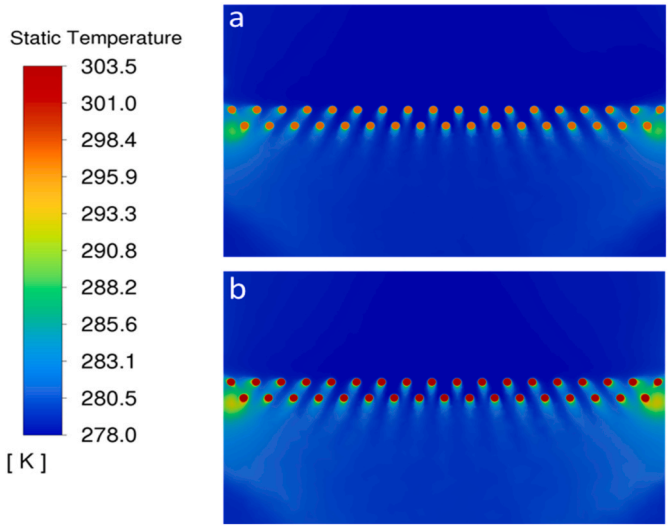

Fig. 16. Pre-heating of incoming air when inlet conditions are 2 m/s and 5 °C (278.15 K) and heat pipe temperature is a) 24 °C (297.15 K) and b) 30 °C (303.15 K).

watts when compared against the baseline case of ventilation with no pre-heating. Energy demand is directly proportional to the temperature difference between the internal room temperature and the fresh air temperature post heat pipes. As a result, the graph produced for energy reduction shows the same trends as shown for pre-heating. At a maximum, a reduction of 860.7 W is achieved using 3 rows of heat pipes at 2 m/s, while at a minimum approximately 114.8 W is saved using 1 row of heat pipes at 4 m/s. By installing heat pipes for heat recovery, the viable operational window of the wind tower is increased. Pre-heating of the incoming air allows the wind tower to be left open longer when ambient temperatures drop whilst limiting any significant increases to heating energy demand.

5. Conclusion and future work

In the context of the COVID-19 pandemic, improving ventilation rates is an increasing concern to limit the spread of indoor pathogens. A method of improving ventilation rates without incurring large increases in energy demand is therefore explored. The results of this study showing that installing horizontally arranged heat pipes through the base of a wind tower did not reduce supply rates below an acceptable range and was simultaneously capable of pre-heating fresh air by up to 2.80 °C.

Further work will look to improve on the performance of the wind tower and heat recovery system. A field test featuring the same wind tower and heat recovery system will allow a comparison between performance in a wind tunnel and real-world conditions. Improvements to performance could be made by introducing a seasonal thermal loop, providing heating and cooling in the winter and summer respectively by storing recovered waste heat for a period of up to 6 months. Through this the potential for pre-heating can be increased, further limiting increased energy demand whilst also recovering a greater amount of waste heat, improving the overall efficiency of the system.

Credit author statement

Harry Mahon: Conceptualisation, Methodology, Software, Validation, Writing – Original Draft, Daniel Friedrich: Writing – Review & Editing, Supervision, Ben Hughes: Writing – Review & Editing, Supervision.

Declaration of competing interest

The authors declare that they have no known competing financial interests or personal relationships that could have appeared to influence the work reported in this paper.

Data availability

Data will be made available on request.

Acknowledgements

This work is funded by the Scottish Research Partnership in Engineering (SRPe-IDP/012) and Free Running Buildings Ltd.

References

[1] IEA. 2019 Global status report for buildings and construction, vol. 224. UN Enviroment programme; 2019. p. 41 [Internet], https://www.iea.org/reports/global-status-report-for-buildings-and-construction-2019. p. Available from:.
[2] International Energy Agency (IEA). The future of cooling opportunities for energy-efficient air conditioning"International energy agency website. 2018. 2018; Available from: www.iea.org.
[3] CIBSE Guide A. Environmental design. Chartered Institution of Building Service Engineers London; 2015.
[4] Jomehzadeh F, Nejat P, Calautit JK, Yusof MBM, Zaki SA, Hughes BR, et al. A review on windcatcher for passive cooling and natural ventilation in buildings, Part 1: indoor air quality and thermal comfort assessment. Renew Sustain Energy Rev 2017;70(October 2016):736–56.
[5] Walker IS, Wilson DJ. Evaluating models for superposition of wind and stack effect in air infiltration. Build Environ 1993;28(2):201–10.
[6] Calautit JK, Hughes BR, O'Connor D, Shahzad SS. Numerical and experimental analysis of a multi-directional wind tower integrated with vertically-arranged heat transfer devices (VHTD). Applied Energy; 2017.
[7] O'Connor D, Calautit JK, Hughes BR. A novel design of a desiccant rotary wheel for passive ventilation applications, vol. 179. Applied Energy [Internet; 2016. p. 99–109. https://doi.org/10.1016/j.apenergy.2016.06.029. Available from:.
[8] Saadatian O, Haw LC, Sopian K, Sulaiman MY. Review of windcatcher technologies [Internet] Renew Sustain Energy Rev 2012;16(3):1477–95. Available from: https://dx.doi.org/10.1016/j.rser.2011.11.037.
[9] Xu Q, Riffat S, Zhang S. Review of heat recovery technologies for building applications, vol. 12. Energies. MDPI AG; 2019.
[10] O'connor D, Calautit JKS, Hughes BR. A review of heat recovery technology for passive ventilation applications, vol. 54. Renewable and Sustainable Energy Reviews; 2016. p. 1481–93. https://doi.org/10.1016/j.rser.2015.10.039 [Internet]. Available from: https://doi.org/10.1016/j.rser.2015.10.039.
[11] Hughes BR, Mak CM. A study of wind and buoyancy driven flows through commercial wind towers. Energy and Buildings [Internet] 2011;43(7):1784–91. https://doi.org/10.1016/j.enbuild.2011.03.022. Available from:.
[12] Calautit JK, Hughes BR. Measurement and prediction of the indoor airflow in a room ventilated with a commercial wind tower, vol. 84. Energy and Buildings; 2014. p. 367–77. https://doi.org/10.1016/j.enbuild.2014.08.015 [Internet]. Available from: https://doi.org/10.1016/j.enbuild.2014.08.01.
[13] Mahon H, O'Connor D, Friedrich D, Hughes B. A review of thermal energy storage technologies for seasonal loops, vol. 239; 2022, 122207. https://doi.org/10.1016/j.energy.2021.122207. Energy [Internet]. Available from: https://doi.org/10.1016/j.energy.2021.122207.
[14] Calautit JK, Hughes BR. Integration and application of passive cooling within a wind tower for hot climates. HVAC R Res 2014;20(7):722–30.
[15] Calautit JK, O'Connor D, Hughes BR. A natural ventilation wind tower with heat pipe heat recovery for cold climates, vol. 87. Renewable Energy [Internet; 2016. p. 1088–104. https://doi.org/10.1016/j.renene.2015.08.026. Available from:.
[16] Calautit J, O'Connor D, Shahzad S, Calautit K, Hughes B. Numerical and experimental analysis of a natural ventilation windcatcher with passive heat recovery for mild-cold climates. In: Energy procedia; 2019.
[17] Akeiber H, Nejat P, Majid MZA, Wahid MA, Jomehzadeh F, Zeynali Famileh I, et al. A review on phase change material (PCM) for sustainable passive cooling in building envelopes. Renewable and Sustainable Energy Reviews; 2016.
[18] Vivian DP, Samuel S, Dejan M, Keqin Y, Dimitris MM, Tom L. Performance of a natural ventilation system with heat recovery in UK classrooms: an experimental study. Energy and Buildings; 2018.
[19] Zender–świercz E. A review of heat recovery in ventilation. Energies 2021;14(6).
[20] Kalantar V. Numerical simulation of cooling performance of wind tower (Baud-Geer) in hot and arid region. Renew Energy 2009;34:246–54.
[21] Calautit JK, Chaudhry HN, Hughes BR, Ghani SA. Comparison between evaporative cooling and a heat pipe assisted thermal loop for a commercial wind tower in hot and dry climatic conditions, vol. 101. Applied Energy [Internet; 2013. p. 740–55. https://doi.org/10.1016/j.apenergy.2012.07.034. Available from:.
[22] Shao L, Riffat SB. Flow loss caused by heat pipes in natural ventilation stacks. Appl Therm Eng 1997;17(4):393–9.
[23] Riffat SB, Gan G. Determination of effectiveness of heat-pipe heat recovery for naturally-ventilated buildings. Appl Therm Eng 1998;18(3–4):121–30.
[24] Hughes BR, Chaudhry HN, Calautit JK. Passive energy recovery from natural ventilation air streams, vol. 113. Applied Energy [Internet; 2014. p. 127–40. https://doi.org/10.1016/j.apenergy.2013.07.019. Available from:.
[25] Alizadehdakhel A, Rahimi M, Alsairafi AA. CFD modeling of flow and heat transfer in a thermosyphon. Int Commun Heat Mass Tran 2010;37(3):312–8.
[26] Hughes BR, Chaudhry HN, Calautit JK. Passive energy recovery from natural ventilation air streams, vol. 113. Applied Energy [Internet; 2014. p. 127–40. https://doi.org/10.1016/j.apenergy.2013.07.019. Available from:.
[27] Mroue H, Ramos JB, Wrobel LC, Jouhara H. Experimental and numerical investigation of an air-to-water heat pipe-based heat exchanger, vol. 78. Applied Thermal Engineering; 2015. p. 339–50 [Internet]. Available from: https://dx.doi.org/10.1016/j.applthermaleng.2015.01.005.
[28] Ramos J, Chong A, Jouhara H. Experimental and numerical investigation of a cross flow air-to-water heat pipe-based heat exchanger used in waste heat recovery. Int J Heat Mass Trans 2016;102:1267–81.
[29] Claudia Klein A, Bartholomay S, Marten D, Lutz T, Pechlivanoglou G, Navid Nayeri C, et al. About the suitability of different numerical methods to reproduce model wind turbine measurements in a wind tunnel with a high blockage ratio. Wind Energy Sci 2018 Jan 17;3(1):439–60.
[30] O'Connor D, Calautit J, Hughes BR. Effect of rotation speed of a rotary thermal wheel on ventilation supply rates of wind tower system, vol. 75; 2015. https://doi.org/10.1016/j.egypro.2015.07.432. Energy Procedia [Internet]. 1705–10. Available from:.
[31] Montazeri H. Experimental and numerical study on natural ventilation performance of various multi-opening wind catchers. Build Environ 2011;46(2):370–8. https://doi.org/10.1016/j.buildenv.2010.07.031 [Internet]. Available from:.
[32] Ansys. ANSYS. FLUENT theory Guide. 2020;(January.
[33] Calautit JK, Tien PW, Wei S, Calautit K, Hughes B. Numerical and experimental investigation of the indoor air quality and thermal comfort performance of a low energy cooling windcatcher with heat pipes and extended surfaces. Renew Energy 2020;145:744–56.
[34] Salim SM, Cheah SC. Wall y+ strategy for dealing with wall-bounded turbulent flows. Newswood Ltd.; 2009. p. 2210.
[35] Sofotasiou P. Aerodynamic optimisation of sports stadiums towards wind comfort. 2017;(January. Available from: http://etheses.whiterose.ac.uk/17820/.
[36] Boache PJ. Perspective: a method for uniform reporting of grid refinement studies. J Fluids Eng Transac ASME 1994;116(3):405–13.
[37] Roache PJ. Quantification of uncertainty in computational fluid dynamics. Annu Rev Fluid Mech 1997;29:123–60.
[38] Roache PJ. Fundamentals of computational fluid dynamics. 1998.
[39] Stern F, Wilson Rv, Coleman HW, Paterson EG. Comprehensive approach to verification and validation of CFD simulations—Part 1: Methodology and procedures. J Fluids Eng Transac ASME 2001;123(4):793–802.
[40] Chen Q, Srebric J. A procedure for verification, validation, and reporting of indoor environment CFD analyses. HVAC R Res 2002;8(2):201–16.
[41] Connor DO, Calautit JK, Calautit K, Shazad S, Hughes BR, Pantua C. Analysis of a rotary passive heat recovery device for natural ventilation windcatcher. IOP Conf Ser Mater Sci Eng 2019;556(1).
[42] O'Connor D, Calautit JK, Hughes BR. A study of passive ventilation integrated with heat recovery. Energy and Buildings; 2014.
[43] Cheng Y, Lien FS, Yee E, Sinclair R. A comparison of large Eddy simulations with a standard k-ε Reynolds-averaged Navier-Stokes model for the prediction of a fully developed turbulent flow over a matrix of cubes. J Wind Eng Ind Aerod 2003;91(11):1301–28.